



HAL
open science

Are We Heading to the Future of Musculoskeletal Tumor Imaging with Ultra-High Field 7T MRI?

Jean-Camille Mattei, Arthur Varoquaux, Alexandre Fouré, Arnaud Le Troter, Alexandre Rochwerger, Sébastien Salas, Sandrine Guis, Corinne Bouvier, Maxime Guye, Christophe Chagnaud, et al.

► **To cite this version:**

Jean-Camille Mattei, Arthur Varoquaux, Alexandre Fouré, Arnaud Le Troter, Alexandre Rochwerger, et al.. Are We Heading to the Future of Musculoskeletal Tumor Imaging with Ultra-High Field 7T MRI?. *Clinical Oncology and Research*, 2019, pp.1-8. 10.31487/j.COR.2019.6.02 . hal-04075015

HAL Id: hal-04075015

<https://hal.science/hal-04075015v1>

Submitted on 6 Sep 2024

HAL is a multi-disciplinary open access archive for the deposit and dissemination of scientific research documents, whether they are published or not. The documents may come from teaching and research institutions in France or abroad, or from public or private research centers.

L'archive ouverte pluridisciplinaire **HAL**, est destinée au dépôt et à la diffusion de documents scientifiques de niveau recherche, publiés ou non, émanant des établissements d'enseignement et de recherche français ou étrangers, des laboratoires publics ou privés.

Research Article

Are We Heading to the Future of Musculoskeletal Tumor Imaging with Ultra-High Field 7T MRI?

Jean-Camille Mattei^{1,2,3*}, Arthur Varoquaux⁴, Alexandre Fouré³, Arnaud Le Troter³, Alexandre Rochwerger¹, Sébastien Salas⁵, Sandrine Guis⁶, Corinne Bouvier⁷, Maxime Guye³, Christophe Chagnaud⁴ and David Bendahan³

¹Service d'orthopédie Unité 3èmeA, Hôpital Nord, Chemin des Bourrély, 13015 Marseille

²Génétique Médicale et génomique fonctionnelle, Pr Levy UMR S910 Inserm, Université Aix Marseille 2, Faculté Timone, Boulevard Jean Moulin, 13005 Marseille

³Center for Magnetic Résonance in Biology and Medicine, Hôpital de la Timone, Boulevard Jean Moulin, 13005 Marseille

⁴Service de Radiologie, Hôpital de la Conception, Boulevard Baille, 13005 Marseille

⁵Service d'Oncologie Médicale du Pr Duffaud, Hôpital de la Timone, Boulevard Jean Moulin, 13005 Marseille

⁶Service de Rhumatologie, Hôpital Nord, Chemin des Bourrély, 13015 Marseille

⁷Laboratoire d'histo-pathologie du Pr. Figarella-Branger, Hôpital de la Timone, Boulevard Jean Moulin, 13005 Marseille

ARTICLE INFO

Article history:

Received: 01 November, 2019

Accepted: 18 November, 2019

Published: 14 January, 2020

Keywords:

7T MRI

ultra-high field

sarcoma

oncology

tumor assessment

ABSTRACT

Background and objectives: Sarcoma preoperative planning critically depends on MRI, sometimes uninformative when compartments barriers or critical structures are involved.

objective: to prospectively assess the feasibility and the potential of 7T MRI in sarcoma.

Methods: Two patients with femoral chondrosarcoma were CT and MRI (1.5 and 7T) scanned with T1W, T2W, GRE and DTI sequences. Image quality and characteristics of the tumors were compared between these modalities.

Results: In-plane resolution was higher at 7T as compared to 1.5T MRI, tumor delineation was more reliable and soft tissue involvement was clearer. DT imaging and corresponding ADC mapping allowed a clear distinction between edema and tumor and identified tumor involvement of collateral ligament allowing healthy structures sparing with histopathology confirmation. 7T MRI was also able to define cortical reaction as precisely as CT imaging.

Conclusion: Musculoskeletal tumours UHF-MRI is promising. Higher resolution and enhanced signal to noise ratio improved tumoral assessment, infiltration and cortex changes. One could expect this non-radiating technique to replace CT investigation for bone tumours assessment and open new perspectives in the fields of vascular or nerve salvage and response to chemo/radiotherapy. Healthy tissue sparing might be facilitated with impacts on function, complication or reconstruction type.

Introduction

Sarcomas are generally handled by a complete surgical resection and for some histological subtypes, it represents the only therapeutic solution [1, 2]. Curative surgery is commonly targeting a complete removal of the tumor through en-bloc resection which necessarily ends up with the

removal of healthy tissues. This type of surgery is based on a preoperative MRI investigation within a tight cooperation between expert radiologists and surgeons. The main issue for this type of surgery is related to the potential sparing of limb and can be compromised if vessels or nerves are involved by the tumor. On that basis, a proper resection protocol is intended to perform a safe oncological surgery and to spare these structures [2]. Although imaging details provided by MRI

*Correspondence to: Jean-Camille Mattei, Secretariat Orthopedie 3A Pavillon Mistral Hopital Nord, Chemin des Bourrely, 13015 Marseille, France; Tel: +33631502927; Fax: +33491966081; E-mail: mattei.orthopedie@gmail.com

and/or CT-Scan might be helpful, per operative conditions may compromise safe removal and/or create unscheduled technical difficulties [2]. In addition, tumor margins delineation might be a complex task, especially when radiologists and surgeons have to face a tumoral surrounding edema and decide to grade it as inflammatory or tumoral [3].

Although MRI and PET-MRI protocols have been optimized for tumor characterization, residual disease detection or response to chemotherapy evaluation, the issue of margin delineation has been scarcely addressed. Few studies have investigated the potential of diffusion-weighted sequences or contrast injection for margins delineation, however the presence of a surrounding edema is still a concerning issue, often impacting the length and thickness of the resected soft tissues with deleterious consequences on functional results and oncological outcomes [4-13]. In addition, tumor cells have been reported sometimes beyond the MRI limits of the tumor within the edematous area [14]. Resection quality is currently assessed by expert pathologists on the basis of microscopic, immuno-histochemical and molecular analyses [15]. The gold standard of a R0 resection remains one of the strongest prognostic factors and R1 or R2 resections have been linked to poorer outcomes [16, 17]. Recent studies indicated that a 1-mm resection margin would be safe thereby emphasizing the potential interest of high-resolution imaging for the preoperative assessment of sarcoma [18, 19]. This observation has been supported by a study which confirmed that routine MRI was not able to detect fascia infiltration in 1/3 of the cases thereby misleading the surgical resection plan [10]. Ultra-high field MRI (i.e. MRI achieved with magnetic field larger than 3T) has been developed over the last few years. The corresponding higher spatial resolution has been mainly used in the neurological and MSK fields with recognized applications for cartilage and bone micro-architecture [20-23]. To our knowledge, the potential of UHF MRI has been preliminary published in some neoplasms but never been assessed in the field of margins delineation of soft tissue tumors. In the present study, we aimed at reporting a preliminary evaluation of UHF MRI for the pre-operative assessment of malignant bone tumors and discussing its potential impact in this field, based on actual oncology bibliography [24-26].

Patients and Methods

I Patients

Two patients (65 and 68-year-old) prospectively volunteered between June 2018 and August 2018 to take part in the project. Informed consent was obtained from all individual participants included in the study. Both patients had a biopsy-proven localized chondrosarcoma of the distal femur.

II MRI Protocol

As part of the standardized evaluation, both patients had a 1.5T MRI and a CT-scan evaluation while a UHF MRI was performed as part of the present research protocol. The conventional 1.5T MRI protocol (Amira Siemens, Erlangen, Germany) was performed with an 18-element phased array knee coil and included T1-weighted, T2-weighted, and contrast-enhanced T1-weighted images in the coronal, axial, and/or sagittal plane. T1-weighted images (spin echo, TR/TE/number of

excitations (NEX)/in plane resolution = 600 msec/8 msec/1/1.1*0.8 mm) and T2-weighted images (fast spin echo, TR/TE/ flip angle/bandwidth/NEX/in plane resolution = 4600 msec/113 msec/160°/200 kHz/3/0.9*1 mm) were obtained with a 3.5 mm slice thickness and a 3.5 mm interslice gap. CT scan (Aquilion Prime, Canon Medical Systems, Otawara, Japan) was performed using a cranio-caudal helical acquisition. Fixed parameters were used according to the manufacturer recommendations: 80x0.5mm detectors, 40mm collimation, 0.5s rotation time, pitch factor of 0.625, 120Kv tube voltage, auto-exposure of mAs intensity, FC30 soft filter, AIDR-3D enhanced reconstruction.

Regarding the 7T MRI protocol, a GRE sequence was performed in the coronal plane (TR/TE/number of excitations (NEX)/in plane resolution = 80 msec/10 msec/1/0.4*0.4 mm). The DTI was also performed in the coronal plane using an EPI DTI fat-suppressed scheme (TR/TE/number of excitations (NEX)/in plane resolution/b values = 7500 msec/74.8 msec/1/1*1 mm/0-500 s/mm²) as previously described [27]. Uniform regions of interest (ROIs) were manually drawn in different parts of the tumor on the coronal GRE MRI. A rigid registration process was used in order to propagate the corresponding masks to the DT images and the diffusion coefficient was measured in the edematous region, the bone cortex, the endosteum and intra-medullary tumors. A comparative assessment of image quality (1.5T and 7T MRI and CT-scan) was performed by an MSK expert radiologist (CC).

Results

There was no secondary effect to be reported during the UHF MRI scan. In both cases, image resolution was larger at UHF as compared to what is commonly reported in conventional MRI and close to the resolution usually obtained in CT scan. In plane resolutions (mm*mm) were respectively 0.4*0.4, 0.7*0.5, 0.8*0.8 and 1*1 for GRE, T1SE, TIRM and EPI DIFF sequences compared with 1*1, 1.1*0.8 and 0.8*0.6 for T2SE FS, T1SE and T1FS with contrast, respectively. The musculoskeletal expert radiologist did confirm that the tumor delineation was easier in UHF MR images.

Patient A: This patient had a grade-2 chondrosarcoma of the distal femur. As illustrated in figure 1, the distal limits of the tumor were clearly visible at 7T whereas they appeared as a blurry signal at 1.5 T. In addition, the bone marrow change down to the epiphysis was visible at 7T but not at 1.5T. Both tumor and edematous areas could be easily distinguished at 7T but not at 1.5 T (Figure 2), where infiltration of muscle fibers was clearly visible using UHF MRI whereas this was impossible using 1.5 T MRI. The very high resolution offered by UHF MRI allowed us to determine that the cortical was not disrupted and that the tumor was purely intra-osseous. As a further quantitative support, diffusion coefficients measured at 7T on the ADC segmented map were significantly higher in the tumor region as compared to the surrounding edema (Table 1 and Figure 3). This difference allowed a clear distinction to be made between tumoral tissue and inflammatory reaction. Based on the UHF MRI observations and measurements, tumor resection was performed taking into account that the hyper contrasted area was an edematous/inflammatory signal and the surrounding muscles were preserved. According to the pathological evaluation and in agreement with the 7T MRI findings, there was no cortical disruption and no

tumoral tissue was found at the margins, which were considered as wide (R0) by the pathologists (Figure 4).

Table 1: ADC coefficient of zones of interest in Figure 3 according to the same zones delineations. The coefficients were significantly different between tumour (Zone 1) and surrounding edema (Zone 4), $p=0,025$.

Zone	ADC diffusion coeff	SD
Tumor (1)	2,5	+/- 0,6
Endosteum (2)	2,22	+/- 0,4
Cortex (3)	0,6	+/- 0,2
Edema (4)	1,3	+/- 0,2

Patient B: Patient B had a chondrosarcoma localized in the medial condyle of the distal femur. According to the tumor extension, the surgical plan could have been either a partial knee excision or a total knee replacement. Similarly, to what has been observed for Patient A, cortical disruption could be assessed at UHF but not using conventional MRI (Figure 5). The ADC diffusion map quantitatively confirmed (Figure 6) the tumoral nature of the hypersignal around the cortical disruption, indicating soft tissue involvement next to the medial collateral ligament (MCL). On that basis, decision was taken to partially excise the MCL. Based on the sole 1.5T MRI investigation, MCL would

not have been excised and the oncologic outcomes might have been poorer. MCL sheath involvement was later confirmed from histological analyses. Of interest, 7T MRI was also used in order to design a 3D-printed personalized cutting guide which we used to minimize bone resection and to perform a partial knee reconstruction.

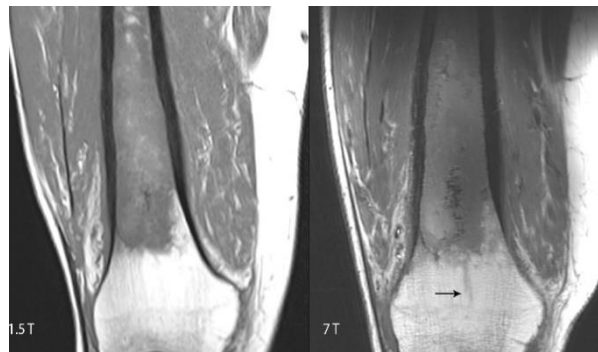


Figure 1: MRI results for Patient A.

Coronal views of distal femur. Left side: T1 TSE sequence using conventional MRI, Right side: T1 TSE sequence using UHF MRI. Tumour delineation, intra-tumoral calcifications, cortex reaction and bone marrow changes are clearer, and UHF MRI was able to detect infiltration going down to the epiphysis and not visible using conventional MRI (arrow).

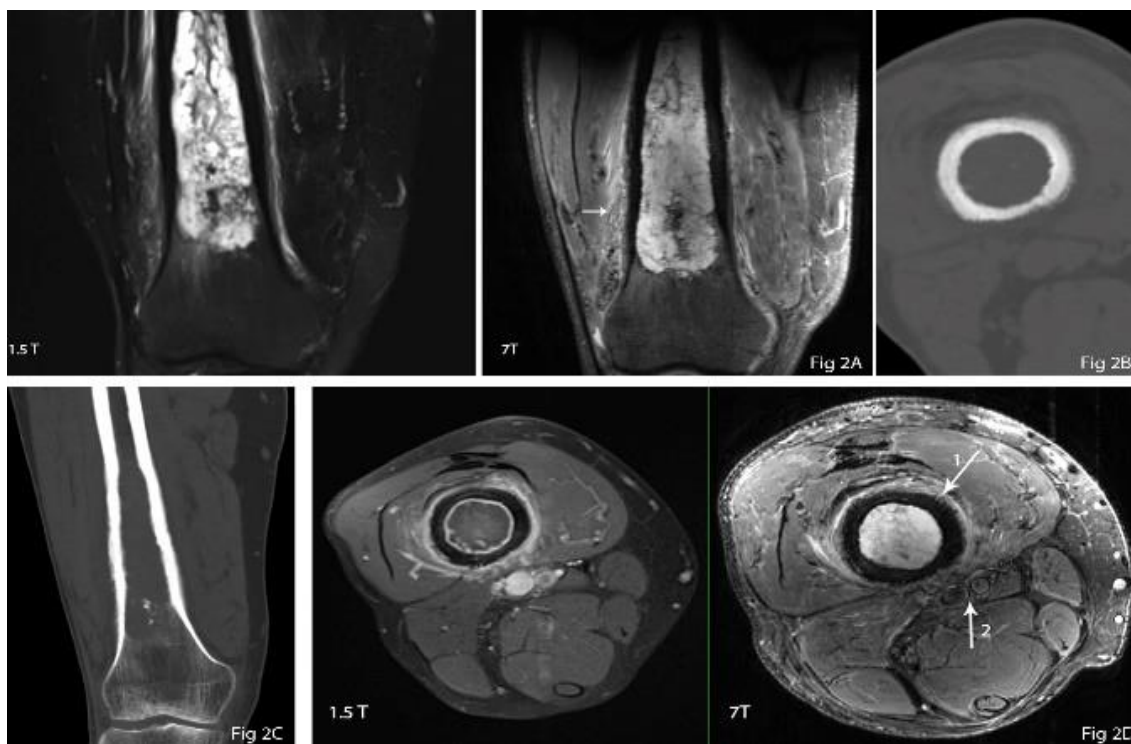


Figure 2A: Coronal views of distal femur. *Left side:* T2 FS sequence using conventional MRI, *Right side:* GRE sequence using conventional UHF MRI. Delineation of the edema through muscle fibres is more visible on UHF MRI (arrow), which would help in cases where distinction between edema and tumour is dubious.

Figure 2B and C: CT scan images (distal femur axial and coronal views, respectively) compared with **Figure 2D** (Axial view of distal femur), *left:* T1 FS after contrast-agent injection, *right:* GRE sequence with UHF MRI. Cortical resolution was equivalent to what can be observed on a CT scan, with visualisation of cortical radiant layers due to tumour growth (arrow 1). Endosteal scalloping was as clear as CT views on UHF MRI and edema analysis was sharper as for Figure 1. Vessels anatomical layers were clear, which will help with future assessment of vascular involvement and surgery planning (arrow 2).

Discussion

Based on this case series, the present results clearly illustrated that UHF MRI outperformed conventional MRI in terms of malignancy characterization, diagnosis and local extension. Advantages of UHF MRI have been already documented in the oncological field, especially in prostate cancer, brain, oesophageal or cervical tumors [28-34]. Non-pathological imaging of bowel has shown increased spatial resolution and interestingly better signal of vessels in abdomen, which seems to be confirmed on our images with clear delineation of vessels anatomical layers [35, 36]. These studies supported the imaging superiority of UHF over conventional MRI. The present study further supports this superiority for sarcomas investigations and illustrates that surgical plan might be optimized. This issue of surgical margins and tumor delineation is of paramount importance in the field of MSK oncology. Margins have been empirically defined considering that fasciae, septa, periosteum or cortical bone would be strong barriers against tumoral involvement of adjacent compartments. However, despite wide excision and safe pathological margins, a substantial recurrence rate has been reported for sarcomas and so most likely because tumoral infiltrations in peri-tumoral edema have been undetected [14, 37]. This would support a low sensitivity of conventional MRI for the detection of tumoral tissue infiltration given that up to one third of fascia tumoral infiltrations could be missed [10]. Diffusion-weighted imaging (DWI) and/or contrast agents have been used to rule out compartments and fasciae involvement. However, contrast to noise ratio of DWI are poor using conventional MRI so that sensitivity or specificity are not improved [10, 11]. The optimization of noise to signal ratio already mentioned in other oncological 7T studies and our preliminary results may suggest that tumor vs. edema distinction could be facilitated in ultra-high field examinations, improving surgical plan, margins and healthy tissue sparing.

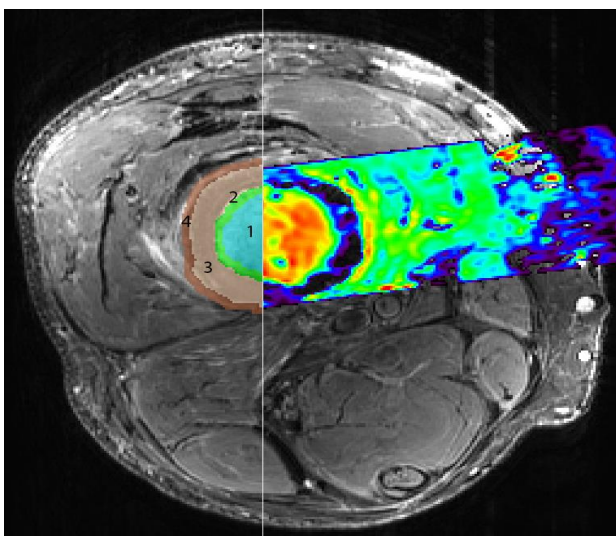


Figure 3: *Left side:* manual segmentation of zones of interest; *right side:* ADC map. All merged with GRE anatomical sequence.

1: tumour, 2: endosteum, 3: cortex, 4: peri-osseous edema;

From a theoretical point of view, a higher magnetic field is expected to provide a better contrast to noise ratio together with a higher resolution. Such a boosting effect has been acknowledged in neurological and MSK

fields but, to our knowledge not in sarcoma surgery [38]. The higher spatial resolution in UHF MR images have been used for the detection of damaged tissues in meniscal or cartilage pathologies and for the investigation of bone microarchitecture [39- 41]. The higher resolution provided by UHF MRI might also change the surgical planning for tumors with a very high infiltrative capacity such as myxofibrosarcoma (MFS), Undifferentiated Pleomorphic Sarcomas (UPS) or epithelioid sarcoma [37, 42]. This remains an ongoing issue in “tail-like pattern” sarcomas, with high risk of recurrence, poorer prognosis, even with extensive tissue resections [43, 44]. Promising results have been found in abdominal 7T imaging especially regarding vessels analysis, also advocating that contrast injection might become optional in vessels analysis. Sarcoma involving neuro vascular structures will certainly benefit from this technical improvement, especially when vessel resection and/or reconstruction is at stake [36]. Crombé et al. have identified MRI features at 1.5 T such as peritumoral enhancement, the presence of an area compatible with necrosis and heterogeneous signal intensities in T2W images which could be linked to high grade-tumours. One could expect, as previously suggested, that UHF MRI might play a role in sarcoma prognosis analysis and patient outcome assessment [45, 46].

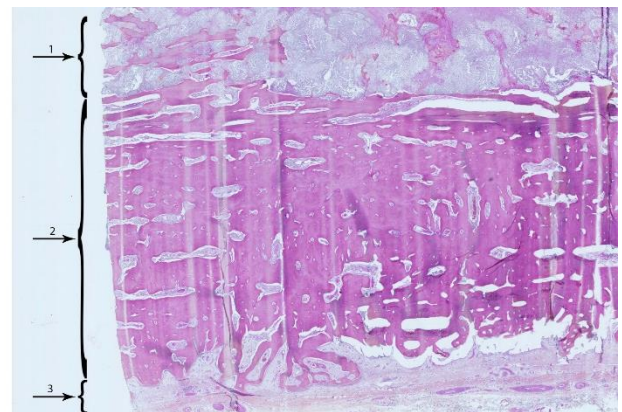


Figure 4: Histopathology slide: endomedullary Grade 2 chondrosarcoma with minimal cortical erosion. The lesion thickened the cortex and no tumoral cells breached into the soft tissues. 1: endosteal tumour, 2: thickened cortex, 3: surrounding muscle, free from tumour involvement;



Figure 5: MRI results for Patient B.

Left: CT scan, coronal view of femoral metaphysis and epiphysis

Middle: UHF MRI coronal view of femoral metaphysis and epiphysis (GRE 3D sequence)

Right: Conventional MRI coronal view of femoral metaphysis and epiphysis (T2 FS sequence).

Cortical disruption can be assessed at UHF MRI and CT but not on the conventional 1.5T MRI. Its detection seems even more precise on UHF MRI than CT (arrows).

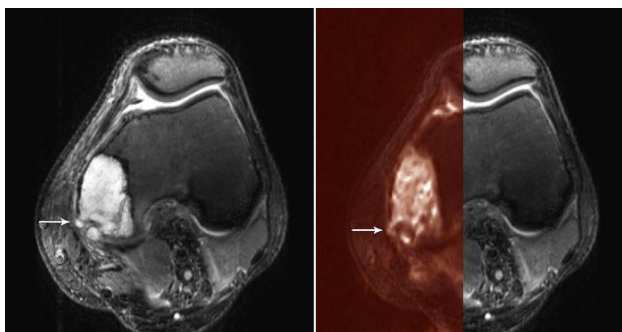


Figure 6: *Left:* GRE axial view of distal femur using UHF MRI. *Right:* ADC map computed from UHF MRI acquisitions and merged on GRE sequence. Postero-lateral cortical disruption and soft tissue close to medial collateral ligament (MCL, arrows) was most probably involved by tumor. ADC map (Right) coefficients comparison confirmed the coefficient to be the same in the tumour than in the soft tissue hypersignal, suggesting the MCL to be involved by the tumour. This was confirmed by histo-pathological analysis

Using conventional MRI, a recent study failed to highlight imaging features of small tumors (<2cm) for which biopsy is difficult [47]. Based on the present results, one can hypothesize that UHF MRI might be helpful. UHF MRI should also play a role for the evaluation of therapeutic strategy (surgical or medical) in sarcoma and also when an additional surgery is planned, and that extensive healthy tissues resection must be prevented. Tumour delineation is also a critical issue in other cancers and previous UHF MRI studies have addressed this issue in glioma and glioblastoma. This approach has been shown safe and feasible for guiding radiation therapy, while offering an enhanced depiction of tumour delineation and possibly modifying tumour target volumes [48-49]. Cell-infiltration is often ill-defined in glioblastoma using contrast-enhanced T1W MRI. Perfusion imaging conducted at UHF illustrated that regions of low tumour infiltration could be probed even in and beyond the oedematous T2 hyperintensity region surrounding macroscopic tumour [50]. UHF anatomical and DW MRI have also been reported as efficient for partial nephrectomy in small renal masses indicating a potential use in perioperative assessment with a maximal sparing of renal parenchyma without compromising oncological outcomes, similarly to sarcoma.

In terms of diagnosis and tumor detection, 7-Tesla MRI has been described as a safe procedure in breast cancer [51]. 3D chemical-exchange saturation transfer imaging (CEST) showed that magnetization transfer asymmetry values were positively correlated with tumor proliferation and that this index might become a biomarker of high interest in breast tumor characterization [52]. In prostate cancer, early detection of adenocarcinoma with discrimination among cancer stages has been reported as possible in mice model using apparent diffusion coefficient (ADC) [53]. In addition, the combination of T2 and Diffusion-weighted imaging might spare contrast injection. A good reproducibility and detection rate using such a combination have been reported [29]. It has also been confirmed that signal to noise ratio (SNR) in 7T images was largely improved (3-fold) as compared to what could be obtained at 3T thereby supporting the superiority of 7T MRI in terms of tumor characterization, tumor aggressiveness staging, tumor metabolism and extra-capsular extension detection. UHF MRI has also

shown interesting results in tumor characterization in brain and prostate. In prostate cancer, $R2^*$ mapping has been used at 7T to assess hypoxemia, a prognosis factor of resistance to therapy. In brain, 7T imaging with short echo-time was found to be useful in the evaluation of the metabolic profile in glioma which could be used as a prognosis factor of treatment efficacy or disease progression [31]. Patch-based super-resolution reconstruction might also be used in high-resolution multi-metabolite mapping of gliomas and in targeted therapies, especially those involving glutamine metabolites. Apart from the superior SNR and CNR, UHF MRI can be used to assess nuclei other than 1H such as ^{23}Na and ^{31}P . Sodium imaging at UHF has been used for assessing IDH mutation status and tumour progression in glioma. On that basis, the new classification approach which has been proposed at early stage, might lead to avoid invasive stereotaxic biopsy and promote individualized patient management [54].

Ultra-high field MRI could also play a major role for the assessment of tumours treatments. It has been shown that 7T MRI could be safely and efficiently used during radiofrequency treatments [55]. More specifically, CEST imaging was able to differentiate viable tumour cells from necrotic areas before and after chemotherapy and so in accordance with histological assessment [56]. Subtle metabolites changes have been detected during chemotherapy using ^{31}P -phosphorus (^{31}P) MRI at UHF so that non responders could be distinguished from partial and complete responders. In brain, CEST imaging performed at 7T was able to distinguish stable and progressive disease under chemo-radiotherapy [57, 58]. Particular attention should however be paid to specific tumour characteristics. For instance, Dreher et al. did find that NOE and Amine Proton Transfer differed between various anatomical brain locations [59]. These studies advocate for a refinement of cell death detection methods and the need of predictive models for response to treatment and for clinical outcomes. In uterine pathology where benign masses might be mistaken with sarcoma, DTI could likely benefit from the superior SNR offered by UHF MRI. Interesting results regarding malignancy characteristics of a given lesion have been reported at 3T [60]. Machine learning might also benefit from technical advances in this field [61, 62].

Conclusion

Considering the spatial resolution of MR images obtained at 7T, UHF-MRI of musculo-skeletal tumours seems very promising. Thanks to the enhanced signal to noise ratio, tumours could be more accurately delimited and distinguished from edema. One can reasonably expect an important impact of UHF-MRI on the surgical planning of sarcoma resection, especially for the sparing of healthy tissues. The present preliminary study confirmed a high potential of UHF-MRI in the field of musculoskeletal tumours and showed that UHF-MRI could play a role for the surgical management of sarcoma. Anatomical GRE sequences could provide an image resolution similar to what could be obtained using CT scan. On that basis, one could expect that for this particular aspect, UHF MRI, a non-radiating technique, could replace the radiating CT-scan investigation. The higher resolution provided by UHF MRI allowed us to uniquely assess the local tumour extension and to clearly assess tumoral infiltration of soft tissues. Such an approach could open new perspectives in the fields of epiphysis preservation in children, vascular or nerve salvage, response to chemotherapy or radiotherapy assessment, detection of tumoral clusters away from the lesion and

muscle resection with an expected large impact on function, complication or reconstruction type. These promising results would have to be confirmed in a larger cohort of patients. All procedures performed in studies involving human participants were in accordance with the ethical standards of the institutional and/or national research committee and with the 1964 Helsinki declaration and its later amendments or comparable ethical standards.

Acknowledgements

The corresponding author would like to thank the Bureau des PU-PH (University Professors Board) of Marseille Medical School and SOFCOT (French Orthopedic Society) for their support.

Synopsis

This study is the first known-to-date Ultra-High Field 7T assessment of sarcoma. This technique allowed a better delineation of tumour margins, bone extension and soft tissue involvement. Signal to noise ratio may allow precise ADC maps and distinction between oedema and tumour extension with future implications in pre-operative planning, neurovascular involvement, response to (neo)adjuvant treatments, tumour characterisation (diagnosis, grade...) and tissue sparing during resection.

Disclosure

The authors have nothing to disclose.

REFERENCES

- VO Lewis (2009) What's new in musculoskeletal oncology. *J Bone Joint Surg Am* 91: 1546-1556. [Crossref]
- MA Smolle, D Andreou, PU Tunn, J Szkandera, B Liegl-Atzwanger, et al. (2017) Diagnosis and treatment of soft-tissue sarcomas of the extremities and trunk. *EFORT Open Rev* 2: 421-431. [Crossref]
- P Lang, G Honda, T Roberts, M Vahlensieck, J O Johnston et al. (1995) Musculoskeletal neoplasm: perineoplastic edema versus tumor on dynamic postcontrast MR images with spatial mapping of instantaneous enhancement rates. *Radiology* 197: 831-839. [Crossref]
- L Bellanova, T Schubert, O Cartiaux, F Lecouvet, C Galant et al. (2014) MRI-Based Assessment of Safe Margins in Tumor Surgery. *Sarcoma* 2014: 686790. [Crossref]
- AM De Schepper, F Vanhoenacker, J Gielen, PM Parizel (2006) Imaging of Soft Tissue Tumors.
- X Zhang, Y LE Chen, R Lim, C Huang, A Chebib et al. (2016) Synergistic role of simultaneous PET/MRI-MRS in soft tissue sarcoma metabolism imaging. *Magn Reson Imaging* 34: 276-279. [Crossref]
- LH Gimber, EA Montgomery, CD Morris, EA Krupinski, LM Fayad (2017) MRI characteristics associated with high-grade myxoid liposarcoma. *Clin Radiol* 72: 613.e1-613.e6. [Crossref]
- L Wang, J Pretell-Mazzini, DA Kerr, L Chelala, X Yang et al. (2018) MRI findings associated with microscopic residual tumor following unplanned excision of soft tissue sarcomas in the extremities. *Skeletal Radiol* 47: 181-190. [Crossref]
- H Choi (2017) Role of Imaging in Response Assessment and Individualised Treatment for Sarcomas. *Clin Oncol R Coll Radiol* 29: 481-488. [Crossref]
- MA Yoon, CG Chee, HW Chung, JS Song, JS Lee et al. (2019) Added value of diffusion-weighted imaging to conventional MRI for predicting fascial involvement of soft tissue sarcomas. *Eur Radiol* 29: 1863-1873. [Crossref]
- S Iwata, A Araki, H Funatsu, T Yonemoto, H Kamoda et al. (2018) Optimal surgical margin for infiltrative soft tissue sarcomas: Assessing the efficacy of excising beyond the infiltration. *J Surg Oncol* 118: 525-531. [Crossref]
- A Tanaka, Y Yoshimura, K Aoki, M Okamoto, M Kito et al. (2017) Prediction of muscle strength and postoperative function after knee flexor muscle resection for soft tissue sarcoma of the lower limbs. *Orthop Traumatol Surg Res* 103: 1081-1085. [Crossref]
- K Harati, J Kolbenshlag, J Bohm, H Niggemann, H Joneidi-Jafari et al. (2018) Long-term outcomes of patients with soft tissue sarcoma of the chest wall: Analysis of the prognostic significance of microscopic margins. *Oncol Lett* 15: 2179-2187. [Crossref]
- LM White, JS Wunder, RS Bell, B O'Sullivan, C Catton et al. (2005) Histologic assessment of peritumoral edema in soft tissue sarcoma. *Int J Radiat Oncol Biol Phys* 61: 1439-1445. [Crossref]
- BP Rubin, CDM Fletcher, C Inwards, AG Montag, T Peabody et al. (2006) Protocol for the examination of specimens from patients with soft tissue tumors of intermediate malignant potential, malignant soft tissue tumors, and benign/locally aggressive and malignant bone tumors. *Arch Pathol Lab Med* 130: 1616-1629. [Crossref]
- E Stoeckle, H Gardet, JM Coindre, G Kantor, F Bonichon et al. (2006) Prospective evaluation of quality of surgery in soft tissue sarcoma. *Eur J Surg Oncol* 32: 1242-1248. [Crossref]
- GK Zagars, MT Ballo, PWT Pisters, RE Pollock, SR Patel et al. (2003) Surgical margins and resection in the management of patients with soft tissue sarcoma using conservative surgery and radiation therapy. *Cancer* 97: 2544-2553. [Crossref]
- V Kainhofer, MA Smolle, J Szkandera, B Liegl-Atzwanger, W Maurer-Ertl et al. (2016) The width of resection margins influences local recurrence in soft tissue sarcoma patients. *Eur J Surg Oncol* 42: 899-906. [Crossref]
- KR Gundle, L Kafchinski, S Gupta, AM Griffin, BC Dickson et al. (2018) Analysis of Margin Classification Systems for Assessing the Risk of Local Recurrence After Soft Tissue Sarcoma Resection. *J Clin Oncol* 36: 704-709. [Crossref]
- KM Friedrich, A Komorowski, S Trattinig (2012) 7T imaging of the wrist. *Semin Musculoskelet Radiol* 16: 88-92. [Crossref]
- NK Bangerter, MD Taylor, GJ Tarbox, AJ Palmer, DJ Park (2016) Quantitative techniques for musculoskeletal MRI at 7 Tesla. *Quant Imaging Med Surg* 6: 715-730. [Crossref]
- O Kraff, A Fischer, AM Nagel, C Mönninghoff, ME Ladd (2015) MRI at 7 Tesla and above: demonstrated and potential capabilities. *J Magn Reson Imaging* 41: 13-33. [Crossref]
- S Trattinig, S Zbýň, B Schmitt, K Friedrich, V Juras et al. (2012) Advanced MR methods at ultra-high field (7 Tesla) for clinical musculoskeletal applications. *Eur Radiol* 22: 2338-2346. [Crossref]
- M Durand, M Jain, B Robinson, E Aronowitz, Y El Douahy et al. (2017) Magnetic resonance microscopy may enable distinction between normal histomorphological features and prostate cancer in the resected prostate gland. *BJU Int* 119: 414-423. [Crossref]
- S Gruber, L Minarikova, K Pinker, O Zaric, M Chmelik et al. (2016) Diffusion-weighted imaging of breast tumours at 3 Tesla and 7 Tesla :

- a comparison. *Eur Radiol* 26: 1466-1473. [[Crossref](#)]
26. G Verma, S Mohan, MP Nasrallah, S Brem, JYK Lee et al. (2016) Non-invasive detection of 2-hydroxyglutarate in IDH-mutated gliomas using two-dimensional localized correlation spectroscopy (2D L-COSY) at 7 Tesla. *J Transl Med* 14: 274. [[Crossref](#)]
 27. A Fouré, AC Ogier, A Le Troter, C Vilmen, T Feiweier et al. (2018) Diffusion Properties and 3D Architecture of Human Lower Leg Muscles Assessed with Ultra-High-Field-Strength Diffusion-Tensor MR Imaging and Tractography: Reproducibility and Sensitivity to Sex Difference and Intramuscular Variability. *Radiology* 287: 592-607. [[Crossref](#)]
 28. H Hu, Y Zhang, S Shukla, Y Gu, X Yu et al. (2017) Dysprosium-Modified Tobacco Mosaic Virus Nanoparticles for Ultra-High-Field Magnetic Resonance and Near-Infrared Fluorescence Imaging of Prostate Cancer. *ACS Nano* 11: 9249-9258. [[Crossref](#)]
 29. D Hausmann, N Aksöz, J von Hardenberg, T Martini, N Westhoff et al. (2018) Prostate cancer detection among readers with different degree of experience using ultra-high b-value diffusion-weighted Imaging: Is a non-contrast protocol sufficient to detect significant cancer? *Eur Radiol* 28: 869-876. [[Crossref](#)]
 30. MW Lagemaat, TWJ Scheenen (2014) Role of high-field MR in studies of localized prostate cancer. *NMR Biomed* 27: 67-79. [[Crossref](#)]
 31. Y Li, M Lafontaine, S Chang, SJ Nelson (2018) Comparison between Short and Long Echo Time Magnetic Resonance Spectroscopic Imaging at 3T and 7T for Evaluating Brain Metabolites in Patients with Glioma. *ACS Chem Neurosci* 9: 130-137. [[Crossref](#)]
 32. EC Obusez, M Lowe, SH Oh, I Wang, Jennifer Bullen et al. 7T MR of intracranial pathology: Preliminary observations and comparisons to 3T and 1.5T. *NeuroImage* 168: 459-476. [[Crossref](#)]
 33. I Yamada, N Miyasaka, K Hikishima, Y Tokairin, T Kawano et al. (2015) Ultra-high-resolution MR imaging of esophageal carcinoma at ultra-high field strength (7.0T) ex vivo : correlation with histopathologic findings. *Magn. Reson. Imaging* 33: 413-419. [[Crossref](#)]
 34. JP Hoogendam, IML Kalleveen, CSA de Castro, AJE Raaijmakers, RHM Verheijen et al. (2017) High-resolution T2-weighted cervical cancer imaging: a feasibility study on ultra-high-field 7.0-T MRI with an endorectal monopole antenna. *Eur Radiol* 27: 938-945. [[Crossref](#)]
 35. ML Hahnemann, O Kraff, S Maderwald, S Johst, S Orzada et al. (2016) Non-enhanced magnetic resonance imaging of the small bowel at 7 Tesla in comparison to 1.5 Tesla : First steps towards clinical application. *Magn Reson Imaging* 34: 668-673. [[Crossref](#)]
 36. A Laader, K Beiderwellen, O Kraff, S Maderwald, K Wrede et al. (2017) 1.5 versus 3 versus 7 Tesla in abdominal MRI : A comparative study. *PLoS One* 12: e0187528. [[Crossref](#)]
 37. KR Gundle, S Gupta, L Kafchinski, AM Griffin, RA Kandel et al. (2017) An Analysis of Tumor- and Surgery-Related Factors that Contribute to Inadvertent Positive Margins Following Soft Tissue Sarcoma Resection. *Ann Surg Oncol* 24: 2137-2144. [[Crossref](#)]
 38. S Trattinig, E Springer, W Bogner, G Hangel, B Strasser et al. (2018) Key clinical benefits of neuroimaging at 7T. *NeuroImage* 168: 477-489. [[Crossref](#)]
 39. G Chang, M Diamond, G Nevsky, RR Regatte, DS Weiss (2014) Early knee changes in dancers identified by ultra-high-field 7 T MRI. *Scand J Med Sci Sports* 24: 678-682. [[Crossref](#)]
 40. E Springer, K Bohndorf, V Juras, P Szomolanyi, Š Zbýň et al. (2017) Comparison of Routine Knee Magnetic Resonance Imaging at 3 T and 7 T. *Invest Radiol* 52: 42-54. [[Crossref](#)]
 41. D Guenoun, A Fouré, M Pithioux, S Guis, T Le Corroller et al. (2017) Correlative Analysis of Vertebral Trabecular Bone Microarchitecture and Mechanical Properties: A Combined Ultra-high Field (7 Tesla) MRI and Biomechanical Investigation. *Spine* 42: E1165-E1172. [[Crossref](#)]
 42. MB McCarville, SC Kao, TV Dao, C Gaffney, CM Coffin et al. (2019) Magnetic resonance and computed tomography imaging features of epithelioid sarcoma in children and young adults with pathological and clinical correlation: a report from Children's Oncology Group study ARST0332. *Pediatr Radiol* 49: 922-932. [[Crossref](#)]
 43. K Kikuta, D Kubota, A Yoshida, H Morioka, Y Toyama et al. (2015) An analysis of factors related to the tail-like pattern of myxofibrosarcoma seen on MRI. *Skeletal Radiol* 44: 55-62. [[Crossref](#)]
 44. Morii T, Tajima T, Honya K, Aoyagi T, Ichimura S (2018) Clinical significance of the tail-like pattern in soft-tissue sarcomas on magnetic resonance imaging. *J Orthop Sci* 23: 1032-1037. [[Crossref](#)]
 45. T Fukuda, K Wengler, R de Carvalho, P Boonsri, ME Schweitzer (2019) MRI biomarkers in osseous tumors, *J Magn Reson Imaging JMRI* 50: 702-718. [[Crossref](#)]
 46. S Ahlawat, J Fritz, CD Morris, LM Fayad (2019) Magnetic resonance imaging biomarkers in musculoskeletal soft tissue tumors: Review of conventional features and focus on nonmorphologic imaging. *J Magn Reson Imaging* 50: 11-27. [[Crossref](#)]
 47. K Pham, NS Ezuddin, J Pretell Mazzini, TK Subhawong (2019) Small soft tissue masses indeterminate at imaging: histological diagnoses at a tertiary orthopedic oncology clinic. *Skeletal Radiol* 48: 1555-1563. [[Crossref](#)]
 48. I Compter, J Peerlings, DBP Eekers, AA Postma, D Ivanov et al. (2016) Technical feasibility of integrating 7 T anatomical MRI in image-guided radiotherapy of glioblastoma : a preparatory study. *Magma* 29: 591-603. [[Crossref](#)]
 49. S Regnery, BR Knowles, D Paech, N Behl, JE Meissner et al. (2019) High-resolution FLAIR MRI at 7 Tesla for treatment planning in glioblastoma patients. *Radiother Oncol* 130: 180-184. [[Crossref](#)]
 50. A Vallatos, HFI Al-Mubarak, JL Birch, L Gallagher, JM Mullin et al. (2018) Quantitative histopathologic assessment of perfusion MRI as a marker of glioblastoma cell infiltration in and beyond the peritumoral edema region. *J Magn Reson Imaging JMRI* 50: 529-540. [[Crossref](#)]
 51. GLG Menezes, BL Stehouwer, DWJ Klomp, TA van der Velden, MAAJ van den Bosch et al. (2016) Dynamic contrast-enhanced breast MRI at 7T and 3T : an intra-individual comparison study. *SpringerPlus* 5: 13. [[Crossref](#)]
 52. O Zanic, A Farr, E Poblador Rodriguez, V Mlynarik, W Bogner et al. (2019) 7T CEST MRI : A potential imaging tool for the assessment of tumor grade and cell proliferation in breast cancer. *Magn Reson Imaging* 59: 77-87. [[Crossref](#)]
 53. DK Hill, E Kim, JR Teruel, Y Jamin, M Widerøe (2016) Diffusion-weighted MRI for early detection and characterization of prostate cancer in the transgenic adenocarcinoma of the mouse prostate model. *J Magn Reson Imaging JMRI* 43: 1207-1217. [[Crossref](#)]
 54. A Biller, S Badde, A Nagel, JO Neumann, W Wick et al. (2016) Improved Brain Tumor Classification by Sodium MR Imaging: Prediction of IDH Mutation Status and Tumor Progression. *AJNR Am J Neuroradiol* 37: 66-73. [[Crossref](#)]
 55. X Li, JV Rispoli (2019) Toward 7T breast MRI clinical study : safety assessment using simulation of heterogeneous breast models in RF

- exposure. *Magn Reson Med* 81: 1307-1321. [[Crossref](#)]
56. J Klein, WW Lam, GJ Czarnota, GJ Stanisiz (2018) Chemical exchange saturation transfer MRI to assess cell death in breast cancer xenografts at 7T. *Oncotarget* 9: 31490-31501. [[Crossref](#)]
 57. JE Meissner, A Korzowski, S Regnery, S Goerke, J Breitling (2019) Early Response Assessment of Glioma Patients to Definitive Chemoradiotherapy Using Chemical Exchange Saturation Transfer Imaging at 7 T *J Magn Reson Imaging JMRI* 50: 1268-1277. [[Crossref](#)]
 58. S Regnery, S Adeberg, C Dreher, J Oberhollenzer, JE Meissner et al. (2018) Chemical exchange saturation transfer MRI serves as predictor of early progression in glioblastoma patients. *Oncotarget* 9: 28772-28783. [[Crossref](#)]
 59. C Dreher, J Oberhollenzer, JE Meissner, J Windschuh, P Schuenke et al. (2019) Chemical exchange saturation transfer (CEST) signal intensity at 7T MRI of WHO IV^o gliomas is dependent on the anatomic location. *J Magn Reson Imaging JMRI* 49: 777-785. [[Crossref](#)]
 60. P Rahimifar, H Hashemi, M Malek, S Ebrahimi, E Tabibian et al. (2019) Diagnostic value of 3 T MR spectroscopy, diffusion-weighted MRI, and apparent diffusion coefficient value for distinguishing benign from malignant myometrial tumours. *Clin Radio* 74: 571. [[Crossref](#)]
 61. M Malek, M Gity, A Alidoosti, Z Oghabian, P Rahimifar et al. (2019) A machine learning approach for distinguishing uterine sarcoma from leiomyomas based on perfusion weighted MRI parameters. *Eur J Radiol* 110: 203-211. [[Crossref](#)]
 62. M Nakagawa, T Nakaura, T Namimoto, Y Iyama, M Kidoh et al. (2019) Machine Learning to Differentiate T2-Weighted Hyperintense Uterine Leiomyomas from Uterine Sarcomas by Utilizing Multiparametric Magnetic Resonance Quantitative Imaging Features. *Acad Radiol* 26: 1390-1399. [[Crossref](#)]